Med Biol Eng Comput (2012) 50:155–163
DOI 10.1007/s11517-011-0859-3

ORIGINAL ARTICLE

Estimating the time scale and anatomical location of atrial fibrillation spontaneous termination in a biophysical model

Laurent Uldry · Vincent Jacquemet · Nathalie Virag · Lukas Kappenberger · Jean-Marc Vesin

Received: 11 August 2011 / Accepted: 23 November 2011 / Published online: 21 January 2012

Abstract Due to their transient nature, spontaneous terminations of atrial fibrillation (AF) are difficult to investigate. Apparently, confounding experimental findings about the time scale of this phenomenon have been reported, with values ranging from 1 s to 1 min. We propose a biophysical modeling approach to study the mechanisms of spontaneous termination in two models of AF with different levels of dynamical complexity. 8 s preceding spontaneous terminations were studied and the evolution of cycle length and wavefront propagation were documented to assess the time scale and anatomical location of the phenomenon. Results suggest that termination mechanisms are dependent on the underlying complexity of AF. During simulated AF of low complexity, the total process of spontaneous termination lasted 3,200 ms and was triggered in the left atrium 800 ms earlier than in the right atrium. The last fibrillatory activity was observed more often in the right atrium. These asymmetric termination mechanisms in both time and space were not observed during spontaneous terminations of complex AF simulations, which showed less predictable termination patterns lasting only 1,600 ms. This study contributes to the interpretation of previous clinical observations, and illustrates how computer modeling provides a complementary approach to study the mechanisms of cardiac arrhythmias.

Keywords Atrial fibrillation · Spontaneous termination · Biophysical modeling

Electronic supplementary material The online version of this article (doi:10.1007/s11517-011-0859-3) contains supplementary material, which is available to authorized users.

L. Uldry (✉) · J.-M. Vesin
Applied Signal Processing Group, Swiss Federal Institute of Technology, EPFL-STI-SCI-JMV, Bâtiment ELD, Station 11, 1015 Lausanne, Switzerland
e-mail: uldrylau@gmail.com

J.-M. Vesin
e-mail: jean-marc.vesin@epfl.ch

V. Jacquemet
Department of Physiology, Université de Montréal, Montréal, Canada

V. Jacquemet
Centre de Recherche, Hôpital du Sacré-Coeur de Montréal, Montréal, Canada

N. Virag
Medtronic Europe, Tolochenaz, Switzerland

L. Kappenberger
University of Lausanne, Lausanne, Switzerland

1 Introduction

Atrial fibrillation (AF) is the most common cardiac arrhythmia. During an AF episode, the upper chambers of the heart (the atria) quiver in a chaotic manner instead of pumping blood effectively. Consequences for patients are discomfort, blood clot formation and high risk of embolic stroke [3]. It was discovered very early that AF episodes could terminate spontaneously, even when the arrhythmia was long-standing [24]. A better understanding of the process of spontaneous AF termination could lead to a more accurate dynamical description of AF, and eventually to the development of more effective therapies. However, the mechanisms of spontaneous AF termination are difficult to study in detail due to their transient nature, and therefore remain poorly understood.

Several clinical studies investigated spontaneous AF termination and illustrated the difficulty to precisely describe the different underlying mechanisms. A study in patients with paroxysmal AF reported that changes in the organization of electrocardiographic signals could be detected up to 1 min prior to AF termination [2]. Another study in paroxysmal AF patients found that changes in the power spectrum of the surface electrocardiogram (ECG) were abrupt and occurred only during the last 1–2 s of the AF episode [5, 16]. During another mapping study of spontaneous AF termination using a basket catheter, the earliest detectable event was observed on average 4 s before termination [15].

Similarly, the spatial patterns of electrical activity leading to AF terminations are not yet fully identified. According to the "multiple wavelet" hypothesis [14], AF might terminate either by a simultaneous block of all fibrillating wavelets, or by a progressive fusion of wavelets into one massive wavefront. In a study based on intra-atrial recordings in humans, observations failed to show any change in number of wavelets or cycle length before spontaneous AF termination, therefore supporting, but not proving, the hypothesis that AF wavelets are simultaneously annihilated [20]. On the other hand, several studies demonstrated that AF global organization or cycle length tended to increase prior to termination, suggesting a process of wavelet fusion [2, 15]. In a mapping study, spontaneous AF termination was found to be polymorphic with spatially heterogeneous groups of unstable rhythms and different dynamical behaviors were observed in the right atrium (RA) and the left atrium (LA) [15]. Taken together, these results underline the need for more accurate dynamical descriptions of the process of spontaneous AF termination.

Computer simulations permit the generation of a high number of spontaneously terminated AF episodes in a much easier way than in clinical settings. A fine analysis of the dynamical mechanisms can be conducted on different temporal and spatial scales, since all variables of interest are accessible over time and space, including the number of fibrillatory wavelets as well as their trajectories and mutual interactions. We previously developed a biophysical model of human atria and studied different dynamical aspects of AF related to its initiation and perpetuation [8], as well as the feasibility of therapeutic strategies for AF [18, 23]. In the present model-based study, we analyzed episodes of spontaneous AF termination to assess the temporal and spatial scales of the mechanisms involved. In order to account for the polymorphic nature of AF, two models of AF with distinct dynamical properties and complexities were investigated, and differences in simulated AF dynamics between the RA and the LA were documented.

2 Methods

2.1 Biophysical models of atrial fibrillation

Different computer models of the atria with realistic anatomy and electrophysiology were developed over the last decade [6, 7, 17, 25]. In order to permit the simulation of long episodes (>1 min) of atrial arrhythmias and therapeutic interventions [17, 18, 23], computational requirements were reduced by simplifying these models. In this study, two biophysical models of AF with an identical anatomical structure but with different cellular kinetics were used to simulate AF dynamics with distinct levels of complexity: (a) a model of meandering AF of type I-II according to the classification of Konings et al. [11], where only a few reentries circulate on the atria, and (b) a model of multiple wavelet AF [14] that could be classified as type-III AF due to the high number of simultaneous reentries.

2.1.1 Atrial geometry and numerical integration

The atrial geometry used in this work is based on slice-by-slice segmentation of human magnetic resonance images, and constructed as a three-dimensional monolayer surface [26]. The resulting geometry included major anatomical obstacles to propagation (Fig. 1). Three-dimensional anatomical structures such as Bachmann's bundle, pectinate muscles or crista terminalis were not included. The atrial surface was discretized using triangular elements (400-μm spatial resolution; 100,000 nodes). A finite volume approach was applied to solve the monodomain propagation equations [19, 26, 27]. Time integration involved operator splitting and adaptive time steps varying in the range 12.5–50 μs [26]. The resulting error in conduction velocity (CV) was lesser than 15% compared to a very fine mesh, but tissue resistivity was adjusted to

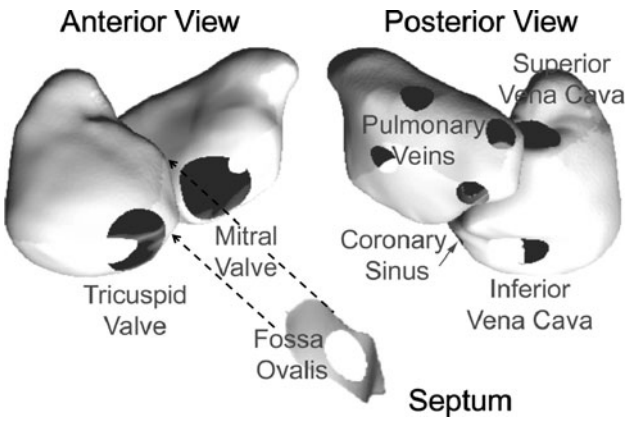

Fig. 1 Geometry of the biophysical model of human atria used in this study: anterior view (on the *left*) and posterior view (on the *right*), with a cut in the septum in the *middle*. The major anatomical obstacles including valves and veins are indicated

compensate for this effect [27]. This parameter adjustment had little effect on tissue excitability and refractoriness. Although this error is significant, such discretization levels are commonly used as a trade-off between accuracy and computational requirements of the numerical problem, and allowed the generation of large amounts of simulations to reproduce clinical observations [12, 18].

2.1.2 Two models of atrial fibrillation

The first model aimed at reproducing low-complexity meandering AF, involving only 1–3 reentries meandering on the atrial surface. A Courtemanche atrial cellular model [4] was used with modified channel conductances to simulate remodeled tissue: the I_{to}, I_{Cal}, and I_{Kur} currents were reduced by 80, 30 and 90%, respectively, and the I_{Kr} current was increased by 50% [7]. These modifications shortened the action potential duration to 210 ms, while reproducing the restitution properties measured in human atrial cells during AF [9]. The atrial substrate was kept homogeneous, and anisotropy of conduction was not considered. The resistivity was set to 500 Ω cm, resulting in a conduction velocity of ~40 cm/s. For this first model, simulated AF was initiated by decremental ramp pacing at the sino-atrial node region, starting at a pacing period of 280 ms, with a 1 ms decrement at each paced beat. The total duration of ramp pacing was 20 s and AF was observed after 9 s.

The second model of AF was based on multiple reentrant wavelets [14]. This type of AF was modeled by a modified Luo–Rudy membrane kinetics model with ionic properties adapted to those of atrial membrane properties ($G_k = 0.423$ mS/cm^2, $G_{Na} = 16$ mS/cm^2, and $G_{si} = 0.085$ mS/cm^2) [8, 13, 26]. This set of parameters constituted the baseline model, in which the mean conduction velocity during sinus rhythm was 70 cm/s (with a resistivity of 200 Ω cm), and the effective refractory period was 260 ms. AF was initiated in the baseline model by 3 s of 20-Hz burst pacing applied near the sino-atrial node. In order to perpetuate AF after initiation by pacing, the model was then adjusted to mimic electrical remodeling as observed in permanent AF by setting $G_{si} = 0.055$ mS/cm^2, resulting in an APD value of 195 ms [8]. This modification allowed us to simulate long-lasting episodes (several minutes) of AF [18]. Such long self-terminating episodes have not yet been obtained in Courtemanche-based models.

2.2 Analysis of spontaneous termination

2.2.1 Database of spontaneous termination episodes

For each model of AF described above, 50 transmembrane potential maps were selected as initial conditions (IC) during the time-course of AF to form an AF database for the study of spontaneous termination. For the model of meandering AF, 50 ICs were taken from 9.6 to 19.4 s after the beginning of ramp pacing, with 200 ms steps. Selecting the instants during pacing ensured that each IC was sufficiently different from the others, and therefore led to distinct termination patterns, since at least one pacing pulse was applied between successive ICs. For the AF model based on multiple wavelets, ICs were taken every 5 s, starting after 30 s of freely evolving AF. In the subsequent simulations, the G_{si} conductance slightly increased to a value of $G_{si} = 0.06$ mS/cm^2 corresponding to paroxysmal AF conditions and enforcing the independence between the ICs with respect to time integration. Following this protocol, two AF databases containing 50 different ICs were created, one for each model of AF. These ICs served as a starting point for the simulation of the 100 AF episodes until spontaneous termination occurred.

2.2.2 Temporal analysis

In order to assess the time scales involved in the AF termination process, the 8-s interval preceding termination was analyzed. AF cycle length (AFCL) was computed as a spatial average of the beat-to-beat intervals measured with 64 electrodes uniformly distributed over the surfaces of both atria (32 on the RA and 32 on the LA). AF dynamics was characterized by two parameters: the number of wavelets present in the atria and the number of wavefronts (#WF). A wavelet was defined as a spatial zone of neighboring atrial cells with a transmembrane potential higher than −60 mV. Wavefronts were defined as depolarizing fronts of wavelets and identified as the zones located at the boundary of a wavelet with a positive derivative of the transmembrane potential. There could be more wavefronts than wavelets since a single wavelet could possibly contain more than one wavefront. The sampling period was 1 ms for AFCL and 5 ms for #WF. A moving average was applied to these signals with a sliding window of 1,000 ms to reduce local fluctuations. Each measure was systematically computed globally in both atria, and separately in the RA and the LA. Statistical comparisons of AFCL and #WF between atria were conducted using Wilcoxon rank sum tests with differences considered to be significant at $p < 0.001$. The time scale of termination τ_{AFCL} was defined as the time between the onset of the last AFCL increase (identified manually) and AF termination; $\tau_{\#WF}$ was defined similarly based on #WF.

2.2.3 Spatial analysis

For each simulation, the location of the extinction sites of the last active reentrant wavefronts before AF termination was identified by visual inspection. In most cases, these last wavefronts were annihilated by one or several collisions,

generating a non-fibrillatory uniform wavefront that died out in one of the extremities of the geometry 200–500 ms later. Extinction sites were defined as locations where the last fibrillatory reentries were blocked by such a collision. A termination pattern was considered to involve a single extinction site whenever the last reentry observed in the tissue was the only remaining one for sufficient period of time T_s before its extinction. Based on preliminary tests, this minimal time interval T_s was defined empirically as 30% of the average AFCL computed across the 50 simulations.

Spatial patterns of spontaneous termination were distinguished according to three different classes of increasing spatial complexity: spontaneous terminations involving (i) a single extinction site, (ii) multiple extinction sites located in the same atrium (denoted as unilateral termination pattern in the RA or the LA), and (iii) multiple extinction sites located in both atria (bilateral termination pattern). All simulations were manually classified. Binomial tests were run to investigate which spatial patterns had a statistically significant tendency to occur more frequently (0.1% significance level).

3 Results

3.1 Duration of simulated atrial fibrillation episodes

Simulations of meandering AF were characterized by a smaller number of fibrillatory wavefronts (6.0 ± 2.8) and a smaller number of wavelets (2.1 ± 0.5) as compared with multiple wavelet AF (7.8 ± 2.7 wavefronts and 5.1 ± 1.4 wavelets; differences were statistically significant, t test $p < 0.01$). Average AFCL of the meandering AF model was 275.0 ± 53.0 ms, whereas the multiple wavelet model had a faster dynamics with an average AFCL of 106.8 ± 39.8 ms. All 100 AF simulations performed in this study self-terminated. Figure 2 shows the histogram of 50 AF episode durations for each AF model. For the meandering AF model, the median episode duration was 7.5 ± 3.9 s, with four episodes lasting much longer than the others (up to 45 s). For the multiple wavelet AF model, the median values for episode duration were 47.1 ± 37.9 s. The range of possible episode durations was much wider than for the meandering AF model (Fig. 2b), and some simulations could be sustained for more than 4 min before spontaneous termination.

3.2 Examples of simulated spontaneous terminations

Figure 3 depicts an example of AF spontaneous termination as simulated by the meandering AF model (for a movie illustrating wavelet dynamics, see Online Resource 1). Simulated AF was characterized by broad wavefronts circulating slowly on the atrial surface, since only 1 to 3 fibrillatory wavelets (translating into approximately 6 wavefronts) could be observed on the tissue, and periods with more than 2 wavelets (e.g. $t = -5{,}470$ ms) were generally short. Approximately 2.5 s before termination, the number of wavelets present in the tissue increased more durably ($t = -2{,}450$ ms). From this point, several collisions between wavefronts progressively decreased the complexity of the global activity ($t = -1{,}310$ ms). A time $t = -790$ ms, several wavefronts were still present in both atria, but a series of conduction blocks occurred due to refractory regions ($t = -710$ ms, blocks indicated by thick red lines). As a result, only one reentry still survived in the RA, while the LA was already free from any fibrillating activity ($t = -460$ ms). The last wave turned rapidly before being blocked by its own refractory tail ($t = -380$ ms, site of extinction indicated by a red star). At this point, no more reentries were present in the tissue, and only a uniform wavefront remained ($t = -290$ ms), propagating from the RA to the LA appendage and finally leaving the tissue free from any activity ($t = -130$ ms).

Figure 4 shows an example of AF spontaneous termination from the AF model of multiple wavelets (for a movie illustrating wavelet dynamics, see Online Resource 2). Between 8 and 3 s before termination, AF was stable and present on the whole atrial surface. The number of fibrillatory wavelets was often above 5, and occasionally up to 10, resulting in a globally installed complex

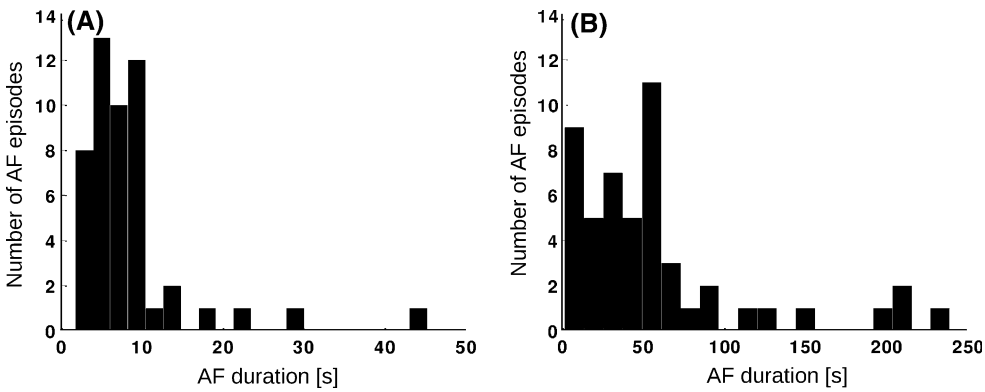

Fig. 2 Histograms of the durations of the 50 episodes of simulated AF for each AF model. **a** Meandering AF model. **b** Multiple wavelet AF model

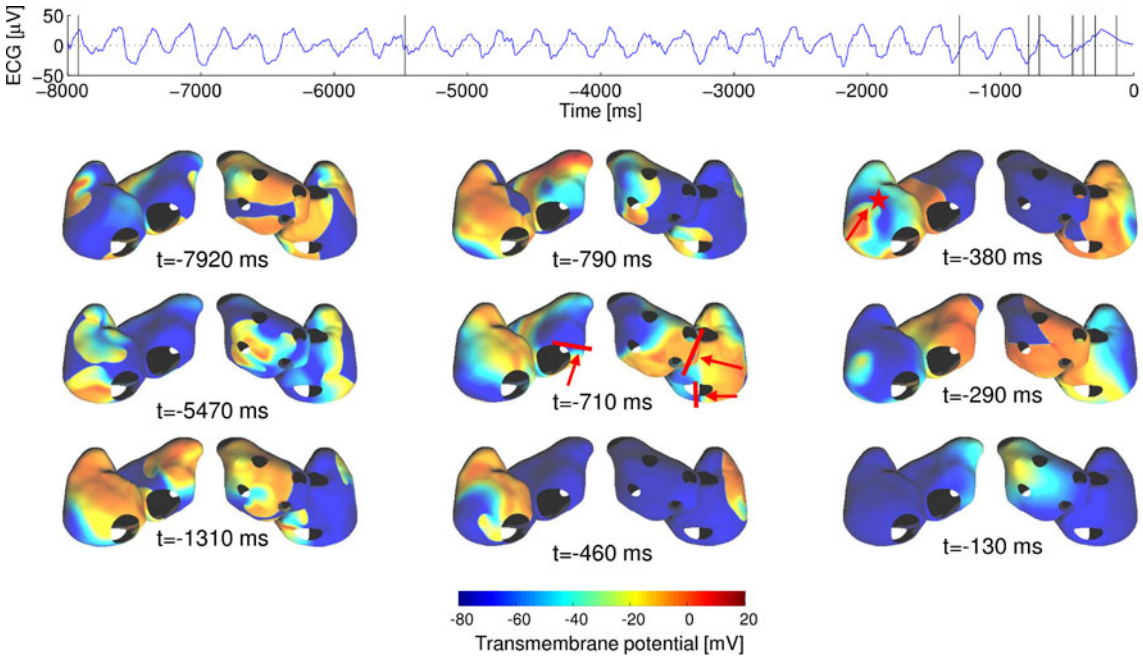

Fig. 3 Maps of transmembrane potentials during simulated meandering AF directly preceding spontaneous termination (see also Online Resource 1). This example corresponds to the 8 s preceding spontaneous termination, and time 0 s corresponds to the exact instant when no more electrical activation is observed on the atria. *Continuous red lines* represent refractory blocks, *red arrows* represent the direction of blocked wavefronts, and the *red star* shows the location of the last extinction site. The *top panel* displays the atrial contribution to the ECG (lead V1). The *vertical bars* represent the time instants of the transmembrane potential maps (colour figure online)

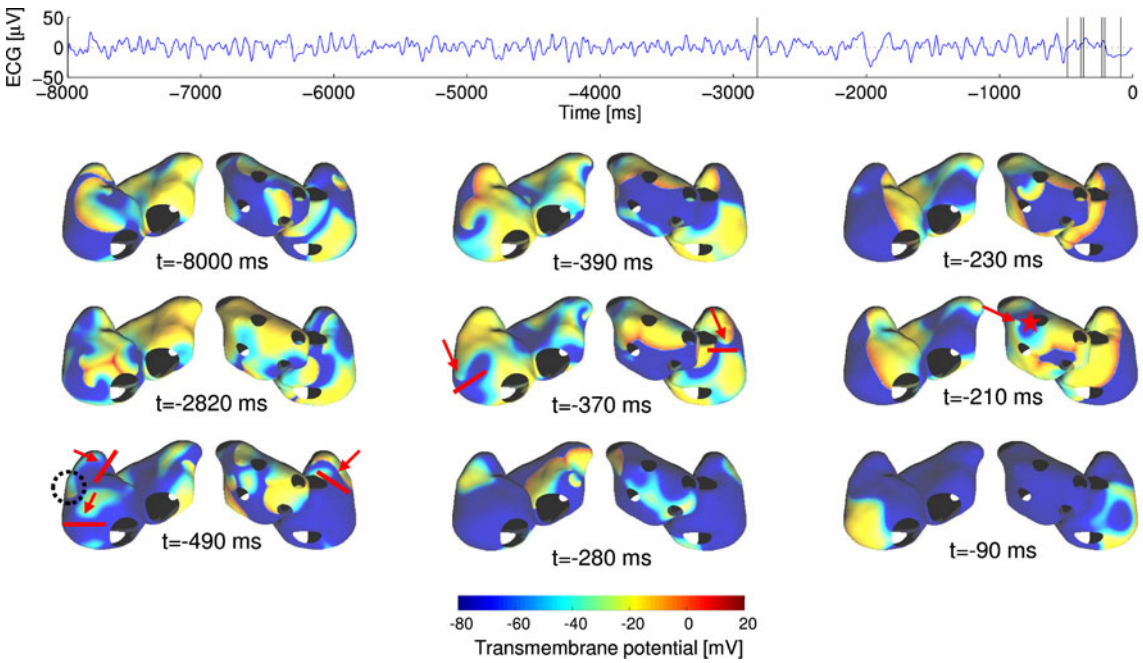

Fig. 4 Maps of transmembrane potentials during simulated multiple wavelet AF directly preceding spontaneous termination (see also Online Resource 2). This example corresponds to the 8 s preceding spontaneous termination, and time 0 s corresponds to the exact instant when no more electrical activation is observed on the atria. *Continuous red lines* represent refractory blocks, *red arrows* represent the direction of blocked wavefronts, and the *red star* shows the location of the last extinction site. The *top panel* displays the atrial contribution to the ECG (lead V1). The *vertical bars* represent the time instants of the transmembrane potential maps (colour figure online)

fibrillating activity. A collision of wavefronts in the LA momentarily depolarizing a major portion of the atrium could be observed 3 s before termination ($t = -2{,}820$ ms). Nevertheless, fibrillating wavefronts still present in the RA rapidly reinitiated AF in both atria and kept it stable for 2 more seconds. The termination process was observed in the 500 last milliseconds, as the number of wavelets progressively decreased. This sudden change was caused by the collision of multiple wavefronts in the RA ($t = -490$ ms). Only one wavelet survived (black dashed circle) and spread into the whole surface of the RA ($t = -390$ ms) before annihilating itself on its refractory tail ($t = -370$ ms), leaving the RA free from any reentry. One or two reentries were still present in the LA ($t = -280$ ms), but tended to be rapidly extinguished through refractory blocks. The last reentry present in the pulmonary veins ($t = -230$ ms) was finally blocked ($t = -210$ ms, site of extinction indicated by a red star), creating a last uniform wavefront propagating from LA to RA before total extinction.

3.3 Temporal analysis of spontaneous terminations

The temporal evolution of AFCL and #WF averaged over the 50 AF termination episodes for the models of meandering AF and multiple wavelet AF is presented in Fig. 5. For the meandering AF model, termination was characterized by a progressive increase in AFCL and decrease in #WF several seconds before AF extinction (Fig. 5a). AFCL started to increase about 3 s before termination globally, but 800 ms earlier in the LA ($\tau_{\mathrm{AFCL}} = 3{,}200$ ms) than in the RA ($\tau_{\mathrm{AFCL}} = 2{,}400$). During these three last seconds, AFCL became significantly higher in the LA than in the RA. In a similar way, #WF started to decrease 1,800 ms earlier in the LA ($\tau_{\#\mathrm{WF}} = 3{,}000$ ms) than in the RA ($\tau_{\#\mathrm{WF}} = 1{,}200$ ms).

Figure 5b depicts the mean temporal evolution of spontaneous termination as observed in the multiple wavelet AF model. Termination was again associated with an increase in AFCL and a sudden decrease in the number

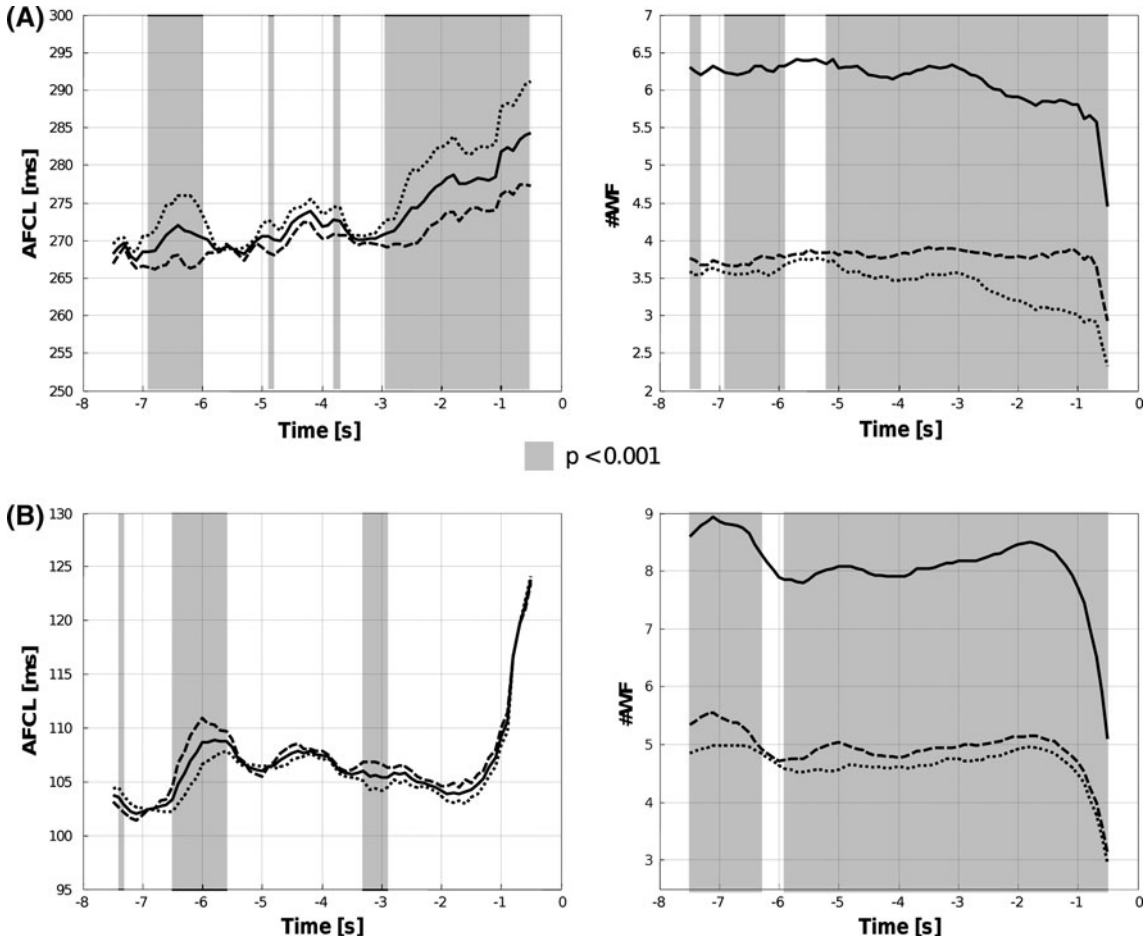

Fig. 5 Mean temporal evolution of AFCL and #WF in both atria (*solid line*), in the RA alone (*dashed line*) and in the LA (*dotted line*) during the 8 s preceding spontaneous termination. Instants when a significant difference ($p < 0.001$) could be observed between the RA and the LA are highlighted in *grey*. **a** Meandering AF model. **b** Multiple wavelet AF model

of wavefronts circulating on the atria, but the timings involved and the overall dynamics were different from the meandering AF model. Dynamical changes in AFCL and #WF triggering termination occurred at the same time in the RA and the LA, and at a shorter time scale compared to the meandering AF model ($\tau_{AFCL} = \tau_{\#WF} = 1{,}600$ ms in both atria). During this termination process, AFCL was similar in the RA and the LA, although AFCL had a tendency to be higher in the RA than in the LA. In addition, there was more than 90% of the time a significantly higher number of wavefronts in the RA than in the LA.

3.4 Spatial analysis of spontaneous terminations

The results of the spatial analysis are summarized in Table 1 and Fig. 6. In the meandering AF model, a clear asymmetry between both atria was found in the spatial distribution of extinction sites. First, it was observed that only five simulations presented termination patterns involving multiple extinction sites located simultaneously on both atria, which represents a significant tendency towards unilateral termination patterns compared to bilateral ones. Moreover, among the 45 unilateral terminations, significantly more extinction sites were located in the RA ($N = 38$) compared to the LA ($N = 7$). While the extinction sites of the LA were randomly distributed over the whole atrium, those located in the RA tended to form clusters around anatomical obstacles (Fig. 6a). This was especially the case in the posterior part of the atrium, where extinction sites were found to create clusters near the inferior and superior vena cava. No preference for termination patterns involving a single or multiple extinction sites could be observed across simulations.

Table 1 Summary of the spatial analysis of spontaneous terminations

	Meandering AF model	Multiple wavelet AF model
Total number of terminations	50	50
Number of terminations in RA	38 (25/13)	25 (14/16)
Number of terminations in LA	7 (5/2)	17 (11/6)
Number of bilateral terminations	5	8
Statistics		
Termination in LA versus RA	$p < 0.001$	NS
Single versus multiple extinction sites	NS	NS
Unilateral versus bilateral terminations	$p < 0.001$	$p < 0.001$

The number of terminations occurring in each atrium and for each AF model is shown. The number of terminations through single/multiple extinction site(s) is given between parenthesis

RA right atrium, *LA* left atrium, *NS* not statistically significant

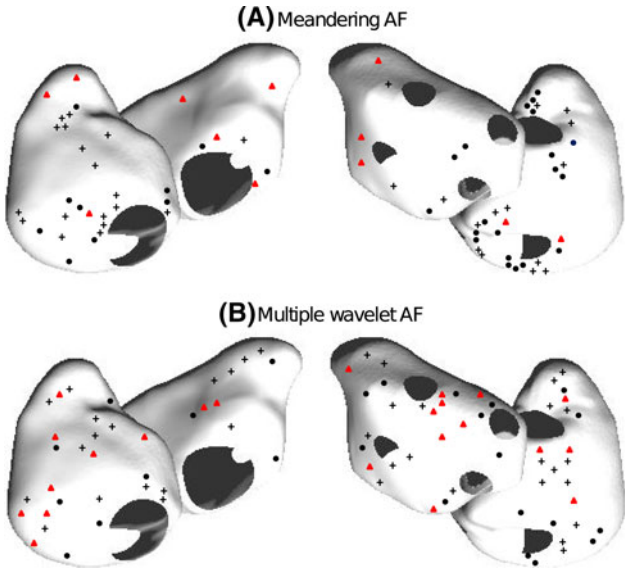

Fig. 6 Spatial distribution of extinction sites for: **a** the model of meandering AF **b** the AF model of multiple wavelet. Spontaneous terminations sites corresponding to single extinction site (*black dots*), multiple extinction sites located on the same atrium (*black crosses*), and multiple extinction sites located on both atria (*red triangles*) are indicated (colour figure online)

The spatial asymmetry in termination dynamics observed in the meandering AF model was not present in the multiple wavelet AF model. Although unilateral terminations were observed significantly more often than bilateral ones, there was no preferred atrial side for termination to occur, as there was no statistical difference in the number of extinction sites observed in each atrium (Table 1). Figure 6b shows that extinction sites were uniformly distributed over the whole atrial surface, so that no cluster of extinction sites possibly indicating a specific termination pattern was found. Finally, there was no statistical preference for single or multiple simultaneous extinction sites, as observed for the meandering AF model.

4 Discussion

Spontaneous termination of AF is difficult to observe, and to investigate in detail. For this reason, only a few studies have tried to describe the mechanisms underlying AF spontaneous termination. This paper proposes a modeling framework providing a detailed description of AF spontaneous termination in both temporal and spatial domains, exploring two models of AF with different dynamics: the type I meandering AF characterized by a low complexity and the multiple wavelet AF with higher complexity (type III).

Our study suggests that spontaneous termination mechanisms may differ depending on the dynamics of the AF

considered, and especially its underlying complexity. This conclusion is in agreement with the clinical and experimental observation that AF complexity increases over time together with AF episode durations [3, 21]. According to our simulation results for low-complexity AF dynamics (meandering AF), spontaneous termination episodes were characterized temporally by a progressive increase in global atrial organization with distinct timings in LA and RA, termination being triggered earlier in the LA. Spatially, the extinction sites of the last observed fibrillatory activity were also asymmetrically distributed, with a bias towards the RA, and a tendency to be clustered around anatomical boundaries. This asymmetry suggests that the LA part of the reentrant circuit followed by the meandering AF driver is critical for AF maintenance. The relative size of the atria and anatomical obstacles may also play a role (the RA is 16% larger than the LA in this model). Due to the small number of driving wavelets, termination often resulted from a collision with its refractory tail.

A temporal decoupling of the atria prior to termination was already reported in clinical observations in human patients with acute or persistent AF, where the earliest detectable event occurred on average 4 s before termination with a significant increase of AFCL in the LA first, followed by an increase in the RA only 1 s later [15]. In the present study, timings for AFCL evolution were similar to those clinical data. In addition, our modeling approach provided information about wavefront propagation. The propensity of extinction sites to be distributed asymmetrically and near anatomical obstacles, however, could not be demonstrated yet in clinical studies, although evidence of interactions between AF waves and anatomical boundaries during AF terminations has already been observed in modeling and experimental studies [1, 10].

Spontaneous terminations in more complex simulated AF such as the multiple wavelet AF took place in a less predictable way and after longer AF duration. Detectable changes before termination occurred only in the last 1–2 s before termination (slightly more than the moving average window length), indicating an abrupt and rapid process. In addition, no difference in timings between LA and RA was observed, or was it possible to find any recurrent spatial pattern in reentry extinctions. This symmetry between LA and RA is interpreted as a consequence of the existence of multiple drivers for AF maintenance both in the LA and the RA. The occurrence of termination through collision between multiple wavefronts was more likely than in the meandering AF model due to a larger number of wavelets and a shorter wavelength.

These findings can be better interpreted in the light of the long-lasting debate about possible mechanisms of AF termination. Whether AF spontaneous termination is preceded by a progressive fusion of wavelets or involves a simultaneous block of all wavelets present in the tissue remains an open question, and past results were mixed. Several studies revealed organization preceding spontaneous terminations [2, 15], while other studies did not [20]. No consensus was found about the appropriate time scale of AF spontaneous termination, ranging from several minutes [2] to 1 s [16]. In both AF models of the present study, terminations at a single or multiple extinction sites were equally likely to be observed. Therefore, the mechanism of simultaneous blocks of multiple wavelets during termination cannot be discarded. Nevertheless, some gradual organization could be observed in both models, although at different degrees depending on AF complexity. In both AF models, spontaneous terminations more often involved extinction sites located in one atrium only. This lateralization of fibrillatory activity prior to termination may be interpreted as an organizing sign, as one of the atrium becomes free of AF before termination occurs. Additional indicators of organization were observed in the meandering AF model, such as the progressive decrease of the number of wavefronts or the progressive increase in global AFCL several seconds before termination. Less complex AF may therefore terminate through more organized mechanisms.

The biophysical models of AF used in this study have several limitations. First, both cell models used in this work only provide approximated AF dynamics. Any further modification of membrane kinetics (through ion channel conductances) may alter AF dynamics, AF duration and the mechanisms of spontaneous termination. The model of multiple wavelet AF presents AFCL values between 100 and 110 ms, which is slightly shorter than reported clinical values for highly complex AF [11]. In contrast, the meandering AF model presents longer AFCL than standard values. Moreover, the models did not include fibrosis or anisotropy. Another limitation is that the atrial geometry was based on a three-dimensional monolayer surface and therefore did not take into account atrial tissue thickness. Several three-dimensional anatomical structures such as Bachmann's bundle, pectinate muscles or crista terminalis were not added to our monolayer geometry. This choice was motivated by the need to assess the effect of more fundamental anatomical structures such as valves or veins on termination. In the case of simulated meandering AF, the observed mechanisms of termination seem to be consistent with what has been reported in the literature. Nevertheless, it should be kept in mind that anatomical structures involved in interatrial communication such as the Bachmann's bundle might have important effects on termination mechanisms under certain conditions. The models of the present study only incorporate electrophysiological properties. Their spontaneous termination mechanisms can only be of electrophysiological origin. Other

aspects, such as electromechanics (e.g. through coughing or intra-atrial blood pressure) or the autonomous nervous system are likely to play a role in the termination process and their time scale may be different.

Our model represents a complementary approach to provide detailed descriptions of spontaneous AF termination under controlled conditions and with sufficient reproducibility. Despite the limitations imposed by their simplifying hypotheses, computer models helped to uncover fundamental mechanisms of cardiac excitations as well as to teach the principles of cardiac electrophysiology [22]. A better understanding of spontaneous AF termination will hopefully lead to new therapeutic approaches that would imitate natural termination by forcing AF activity towards self-termination. As an example, a better description of the spatial patterns preceding spontaneous terminations in AF with low complexity could help finding preferential anatomical areas for terminations to occur. Such knowledge could lead to the development of refined ablation procedures that would constrain fibrillatory wavefronts into a controlled and robust termination process.

Acknowledgments This work was supported by grants from the Theo-Rossi-Di-Montelera Foundation, the Swiss Governmental Commission of Innovative Technologies (CTI), Medtronic Europe, the Natural Sciences and Engineering Research Council of Canada, and the Heart and Stroke Foundation of Québec.

References

1. Agladze K, Kay MW, Krinsky V, Sarvazyan N (2006) Interaction between spiral and paced waves in cardiac tissue. Am J Physiol Heart Circ Physiol 293(1):H503–H513
2. Alcaraz R, Rieta JJ, Hornero F (2008) Non-invasive characterization of atrial activity immediately prior to termination of paroxysmal atrial fibrillation. Rev Esp Cardiol 61(2):154–160
3. Camm AJ, Kirchhof P, Lip GYH, Schotten U, Savelieva I, Ernst S, Gelder ICV, Al-Attar N, Hindricks G, Prendergast B, Heidbuchel H, Alfieri O, Angelini A, Atar D, Colonna P, Caterina RD, Sutter JD, Goette A, Gorenek B, Heldal M, Hohloser SH, Kolh P, Heuzey JYL, Ponikowski P, Rutten FH (2010) Guidelines for the management of atrial fibrillation: the task force for the management of atrial fibrillation of the European Society of Cardiology (ESC). Eur Heart J 31(19):2369–2429
4. Courtemanche M, Ramirez R, Nattel S (1998) Ionic mechanisms underlying human atrial action potential properties: insights from a mathematical model. Am J Physiol 275(1):H301–H321
5. Fujiki A, Sakabe M, Nishida K, Mizumaki K, Inoue H (2003) Role of fibrillation cycle length in spontaneous and drug-induced termination of human atrial fibrillation. Circ J 67(5):391–395
6. Harrild D, Henriquez C (2000) A computer model of normal conduction in the human atria. Circ Res 87:e25–e36
7. Jacquemet V, Virag N, Ihara Z, Dang L, Blanc O, Zozor S, Vesin JM, Kappenberger L, Henriquez C (2003) Study of unipolar electrogram morphology in a computer model of atrial fibrillation. J Cardiovasc Electrophysiol 14:S172–S179
8. Jacquemet V, Virag N, Kappenberger L (2005) Wavelength and vulnerability to atrial fibrillation: insights from a computer model of human atria. Europace 7:S83–S92
9. Kim BS, Kim YH, Hwang GS, Pak HN, Lee SC, Shim WJ, Oh DJ, Ru YM (2002) Action potential duration restitution kinetics in human atrial fibrillation. J Am Coll Cardiol 39:1329–1336
10. Kneller J, Kalifa J, Zou R, Zaitsev AV, Warren M, Berenfeld O, Vigmond EJ, Leon LJ, Nattel S, Jalife J (2005) Mechanisms of atrial fibrillation termination by pure sodium channel blockade in an ionically-realistic mathematical model. Circ Res 96(5):e35–e47
11. Konings KT, Kirchhof CJ, Smeets JR, Wellens HJ, Penn OC, Allessie MA (1994) High-density mapping of electrically induced atrial fibrillation in humans. Circulation 89(4):1665–1680
12. Lines GT, MacLachlan MC, Linge S, Tveito A (2009) Synchronizing computer simulations with measurement data for a case of atrial flutter. Ann Biomed Eng 37:1287–1293
13. Luo CH, Rudy Y (1991) A model of ventricular cardiac action potential. Circ Res 68:1501–1526
14. Moe GK (1962) On the multiple wavelet hypothesis of atrial fibrillation. Arch Int Pharmacodyn Ther 140:183–188
15. Ndrepepa G, Weber S, Karch MR, Schneider MAE, Schömig A, Schmitt C (2002) Electrophysiologic characteristics of the spontaneous onset and termination of atrial fibrillation. Am J Cardiol 90:1215–1220
16. Petrutiu S, Sahakian AV, Swiryn S (2007) Abrupt changes in fibrillatory waves characteristics at the termination of paroxysmal atrial fibrillation in humans. Europace 9(7):466–470
17. Reumann M, Bohnert J, Seeman G, Osswals B, Dössel O (2008) Preventive ablation strategies in a biophysical model of atrial fibrillation based on realistic anatomical data. IEEE Trans Biomed Eng 55:399–406
18. Ruchat P, Dang L, Virag N, von Segesser LK, Kappenberger L (2007) Use of a biophysical model of atrial fibrillation in the interpretation of the outcomes of surgical ablation procedures. Eur J Cardiothorac Surg 32:90–95
19. Shao H, Sampson KJ, Pormann JB, Rose DJ, Henriquez CS (2004) A resistor interpretation of general anisotropic cardiac tissue. Math Biosci 187:155–174
20. Sih HJ, Ropella KM, Swiryn S, Gerstenfeld EP, Sahakian AV (1994) Observations from intraatrial recordings on the termination of electrically induced atrial fibrillation in humans. Pacing Clin Electrophysiol 17:1231–1242
21. Sih HJ, Zipes DP, Berbari EJ, Adams E, Olgin JE (2000) Differences in organization between acute and chronic atrial fibrillation in dogs. J Am Coll Cardiol 36(3):924–931
22. Spector PS, Habel N, Sobel BE, Bates JHT (2011) Emergence of complex behavior: an interactive model of cardiac excitation provides a powerful tool for understanding electrical propagation. Circ Arrhythm Electrophysiol 4(4):586–591
23. Uldry L, Virag N, Vesin JM, Kappenberger L (2010) Optimizing local capture of atrial fibrillation: a model based study of the influence of tissue dynamics on the outcome of rapid pacing. Ann Biomed Eng 38(12):3664–3673
24. Vaisrub S (1950) Spontaneous reversion to normal sinus rhythm in a case of auricular fibrillation of long standing. Can Med Assoc J 63:599–600
25. Vigmond EJ, Tsoi V, Kuo S, Arvalo H, Kneller J, Nattel S, Trayanova N (2004) The effect of vagally induced dispersion of action potential duration on atrial arrhythmogenesis. Heart Rhythm 1:334–344
26. Virag N, Jacquemet V, Henriquez CS, Zozor S, Blanc O, Vesin JM, Pruvot E, Kappenberger L (2002) Study of arrhythmias in a computer model based on magnetic resonance images of human atria. Chaos 12:754–763
27. Zozor S, Blanc O, Jacquemet V, Virag N, Vesin JM, Pruvot E, Kappenberger L, Henriquez CS (2003) A numerical scheme for modeling wavefront propagation on a monolayer of arbitrary geometry. IEEE Trans Biomed Eng 50:412–420